

Combined virtual and experimental screening multicomponent crystals of 2,4- Dichlorophenoxyacetic acid

Jiulong Li^a, Chang Li^a, Xu Ji^a, Qin Sun^b, Zhi Li^c, He Liu^d, Lina Zhou^{a,e}, Dingding

Jing^f, Junbo Gong^{a,e}, Wei Chen^{a,e,*}

^a School of Chemical Engineering and Technology, Tianjin University, Tianjin 300072,
PR China

^b Shenyang Sinochem Agrochemicals R&D Co., Ltd., Shenyang, Liaoning 110021, PR
China

^c School of Pharmaceutical Science and Technology, Tianjin University, Tianjin
300072, PR China

^d Beijing Chao-Yang Hospital affiliated with Beijing Capital Medical University,
Beijing 100020, PR China

^e National Collaborative Innovation Centre of Chemical Science and Engineering,
Tianjin 300072, PR China

^f Asymchem Life Science Tianjin Co., Ltd., Tianjin 300457, PR China

*Corresponding Author, E-mail: chenwei@tju.edu.cn; Tel.: +86-22-2740-5754

Contents

Table S1 The preparation conditions for multicomponent crystals

Table S2 HPLC method parameters for 2,4-D.

Table S3 COSMO-RS calculation and MC analysis results of 2,4-D with coformers.

Table S4 Parameters (Å, Degree) of the hydrogen bonds.

Table S5 Equilibrium solubility of pure 2,4-D and its multicomponent crystals in the water at 25°C.

Table S6 The water solubilities of the coformers of all salts.

Table S7 The pH of a saturated solution at 25°C.

Figure S1 PXRD patterns of LAG experiment product with new phases.

Figure S2 PXRD patterns of LAG experiment product without new phases.

Figure S3 PXRD patterns of multicomponent crystals (black and blue represent the results of slurry suspension experiments and software calculations, respectively).

Figure S4 DSC curves of 2,4-D, (2,4-D)-(PZ)⁺, (2,4-D)-(BZ)⁺, (2,4-D)-(ABA)⁺, (2,4-D)-(PPD)⁺, (2,4-D)-(OPD)⁺, and 2,4-D-EB.

Figure S5 DSC curves of coformers in all multicomponent crystals.

Figure S6 TGA and DSC curves of (2,4-D)-(ABA)⁺.

Figure S7 FTIR spectra of the starting materials and multicomponent crystals.

Figure S8 The PXRD patterns of 2,4-D and multicomponent crystals before (black) and after (blue) equilibrium solubility experiment.

Figure S9 The standard curve of pure 2,4-D solubility.

Figure S10 The PXRD patterns of 2,4-D and multicomponent crystals before (black) and after (blue) accelerated stability experiment.

Figure S11 The MEPs of multicomponent crystals.

Figure S12 Hirshfeld 2D fingerprint plots of 2,4-D and multicomponent crystals.

Table S1 The preparation conditions for multicomponent crystals

Compound	Detail
	slurry suspension method

(2,4-D) ⁻ (PZ) ⁺	2,4-D (884 mg, 4 mmol), PZ (172 mg 2 mmol), methanol (10 ml)
(2,4-D) ⁻ (BZ) ⁺	2,4-D (884 mg, 4 mmol), BZ (472 mg 4 mmol), acetonitrile (10 ml)
(2,4-D) ⁻ (ABA) ⁺	2,4-D (884 mg, 4 mmol), ABA (548 mg 4 mmol), acetonitrile (10 ml)
(2,4-D) ⁻ (PPD) ⁺	2,4-D (884 mg, 4 mmol), PPD (432 mg 4 mmol), ethanol (10 ml)
(2,4-D) ⁻ (OPD) ⁺	2,4-D (884 mg, 4 mmol), OPD (432 mg 4 mmol), methanol (10 ml)
2,4-D-EB	2,4-D (884 mg, 4 mmol), EB (660 mg 4 mmol), methanol (10 ml) slow solvent evaporation method
(2,4-D) ⁻ (PZ) ⁺	2,4-D (88.4 mg, 0.4 mmol), PZ (34.4 mg 0.4 mmol), methanol (4 ml)
(2,4-D) ⁻ (BZ) ⁺	2,4-D (88.4 mg, 0.4 mmol), BZ (47.2 mg 0.4 mmol), acetonitrile (4 ml)
(2,4-D) ⁻ (ABA) ⁺	2,4-D (88.4 mg, 0.4 mmol), ABA (54.8 mg 0.4 mmol), acetonitrile (4 ml)
(2,4-D) ⁻ (PPD) ⁺	2,4-D (88.4 mg, 0.4 mmol), PPD (43.2 mg 0.4 mmol), ethanol (4 ml)
(2,4-D) ⁻ (OPD) ⁺	2,4-D (88.4 mg, 0.4 mmol), OPD (43.2 mg 0.4 mmol), methanol (4 ml)
2,4-D-EB	2,4-D (88.4 mg, 0.4 mmol), EB (66.0 mg 0.4 mmol), methanol (4 ml)

Table S2 HPLC method parameters for 2,4-D.

Parameter	Details
Column	C18 reverse phase column (4.6 mm × 250 mm, 5 µm)
Mobile phase	acetonitrile, water and acetic acid (v/v/v, 50:50:1)
Flow rate	1 mL/min
Inject volume	20 µL
Column temperature	25 °C
Sample temperature	25 °C
λ_{max}	283 nm
Retention time	8.4 min
Calibration range	0.1 – 0.6 g/L

Table S3 COSMO-RS calculation and MC analysis results of 2,4-D with coformers.

	Coformer	CAS No.	ΔH_{ex} (kcal·mol ⁻¹)	Hit Rate (%)	New form
1	piperazine	110-85-0	-5.502	100	yes
2	L-proline	147-85-3	-4.882	100	yes
3	6-aminocaproic acid	60-32-2	-4.762	100	yes
4	gabapentin	60142-96-3	-4.470	0	
5	L-glutamine	56-85-9	-4.103	0	
6	4,4'-bipyridine ¹	553-26-4	-3.920	100	yes
7	L-alanine	56-41-7	-3.570	0	
8	L-valine	72-18-4	-3.480	0	
9	L-histidine	71-00-1	-3.455	0	
10	L-asparagine	70-47-3	-3.396	0	
11	glycine	56-40-6	-3.226	0	
12	creatine	57-00-1	-3.198	0	
13	pyrazine ²	290-37-9	-2.662	100	yes
14	L-threonine	6028-28-0	-2.624	0	
15	imidazole ³	288-32-4	-2.560	100	yes
16	2-ethoxybenzamide	938-73-8	-2.513	100	yes
17	3-aminobenzoic acid	99-05-8	-2.484	100	yes
18	1,2,4-triazole	288-88-0	-2.470	0	
19	2-aminopyrimidine ⁴	109-12-6	-2.409	100	yes
20	methylurea	598-50-5	-2.322	0	
21	<i>p</i> -phenylenediamine	106-50-3	-2.279	100	yes
22	L-serine	56-45-1	-2.164	0	
23	2-aminopyridine ³	504-29-0	-2.129	100	yes
24	benzimidazazole	51-17-2	-2.082	100	yes

25	isonicotinamide ³	1453-82-3	-2.068	100	yes
26	urea	57-13-6	-2.012	0	
27	L-aspartic acid	56-84-8	-2.005	0	
28	pyrazinamide ³	98-96-4	-1.851	100	yes
29	picolinamide	1452-77-3	-1.772	100	yes
30	sulfanilic acid	121-57-3	-1.586	100	no
31	<i>o</i> -phenylenediamine	95-54-5	-1.556	100	yes
32	theophylline	58-55-9	-1.525	100	yes
33	taurine	107-35-7	-1.492	0	
34	mannitol	87-78-5	-1.196	0	
35	6-hydroxypurine	68-94-0	-1.038	100	no
36	2,2'-bipyridine ²	366-18-7	-0.969	100	yes
37	2-hydroxynicotinic acid	609-71-2	-0.840	100	no
38	2-hydroxybenzylamine	932-30-9	-0.620	100	yes
39	oxalic acid	144-62-7	-0.516	0	
40	3-hydroxyisonicotinic acid	10128-71-9	-0.253	100	no
41	3,5-dinitrobenzoic acid	99-34-3	-0.235	0	
42	2-aminonicotinic acid	5345-47-1	-0.202	100	no
43	malic acid	6915-15-7	-0.176	0	
44	malonic acid	141-82-2	-0.137	0	
45	3-aminopyridine ³	462-08-8	-0.085	100	yes
46	2-nitrobenzoic acid	552-16-9	-0.033	0	
47	3-methoxyphenol	150-19-6	0.006		
48	3,4-dihydroxybenzoic acid	99-50-3	0.015		
49	caffeic acid	331-39-5	0.017		
50	2-nitrophenol	88-75-5	0.048		
51	tartaric acid	147-71-7	0.060		

52	saccharin	81-07-2	0.105
53	barbituric acid	67-52-7	0.222

Table S4 Parameters (\AA , Degree) of the hydrogen bonds.

Compound	D-H \cdots A	D-H	H \cdots A	D \cdots A	D-H \cdots A	symmetry
(2,4-D) $^-(\text{PZ})^+$	N ₁ -H _{1A} \cdots O ₁	1.01(2)	1.68(2)	2.681(2)	174(2)	
	N ₁ -H _{1B} \cdots O ₅	0.84(2)	1.94(2)	2.784(19)	179(2)	1-x,-y,1-z
	N ₁ -H _{2A} \cdots O ₄	0.97(2)	1.75(2)	2.715(2)	173(2)	
	N ₂ -H _{2B} \cdots O ₂	0.91(2)	1.80(2)	2.706(19)	172(2)	1-x,1-y,1-z
	C ₄ -H _{4A} \cdots O ₂	0.97	2.37	3.267(2)	153	-x,1-y,1-z
	C ₂ -H _{6B} \cdots O ₅	0.97	2.41	3.289(2)	151	2-x,-y,1-z
(2,4-D) $^-(\text{BZ})^+$	N ₁ -H ₁ \cdots O ₁	0.95(2)	1.70(2)	2.650(16)	177.0(19)	
	N ₁ -H ₁ \cdots O ₂	0.95(2)	2.51(2)	3.069(17)	117.2(16)	3/2-x,-y,-1/2+z
	N ₂ -H ₂ \cdots O ₂	0.89(2)	1.89(2)	2.683(17)	147(2)	-1/2+x,1/2-y,1-z
	C ₉ -H ₇ \cdots O ₂	0.93	2.56	3.087(2)	117	
(2,4-D) $^-(\text{ABA})^+$	N ₁ -H _{1A} \cdots O ₁	0.91(3)	1.86(3)	2.7713(19)	175(2)	
	N ₁ -H _{1B} \cdots O ₅	0.86(3)	2.12(3)	2.690(2)	124(2)	-1/2+x,5/2-y,-1/2+z
	N ₁ -H _{1C} \cdots O ₁	0.90(3)	1.90(3)	2.7762(19)	166(2)	3/2-x,1/2+y,1/2-z
	N ₁ -H _{1C} \cdots O ₂	0.90(3)	2.52(3)	3.132(2)	126.4(19)	3/2-x,1/2+y,1/2-z
	O ₄ -H ₂ \cdots O ₂	0.80(3)	1.84(3)	2.633(2)	169(4)	1/2+x,3/2-y,1/2+z
	C ₁₄ -H ₉ \cdots O ₄	0.93	2.53	3.369(2)	149	x,1+y,z
(2,4-D) $^-(\text{PPD})^+$	C ₁₅ -H ₁₀ \cdots O ₁	0.93	2.48	3.361(2)	159	x,1+y,z
	N ₁ -H _{1A} \cdots O ₂	0.89	1.87	2.724(2)	160	
	N ₁ -H _{1B} \cdots O ₁	0.89	1.86	2.7476(19)	174	2-x,1-y,-z

	N ₁ -H _{1C} ···O ₁	0.89	1.98	2.748(2)	144	1+x,y,z
	C ₉ -H ₆ ···O ₂	0.93	2.53	3.265(2)	136	2-x,1-y,-z
(2,4-D) ⁻ (OPD) ⁺	N ₁ -H _{1A} ···O ₁	0.911(18)	0.911(18)	2.7378(13)	156.1(16)	
	N ₁ -H _{1B} ···O ₂	0.922(16)	1.957(16)	2.8448(13)	161.1(14)	1-x,-1/2+y,1/2-z
	N ₁ -H _{1C} ···O ₂	0.929(15)	1.929(15)	2.8220(14)	160.7(13)	x,3/2-y,1/2+z
	N ₂ -H _{2A} ···O ₁	0.870(18)	2.068(18)	2.9301(15)	170.6(14)	x,3/2-y,1/2+z
2,4-D-EB	O ₁ -H ₁ ···O ₄	0.94(3)	1.64(3)	2.578(2)	175(4)	
	N ₁ -H _{2A} ···O ₂	0.90(3)	2.01(3)	2.887(3)	166(3)	
	N ₁ -H _{2B} ···O ₅	0.94(4)	1.87(3)	2.633(3)	137(4)	
	C ₈ -H ₆ ···O ₄	0.93	2.57	3.478(4)	164	1/2-x,-1/2+y,3/2-z
	C ₁₅ -H ₁₀ ···O ₄	0.93	2.37	2.719(3)	102	
	C ₁₇ -H _{12A} ···O ₂	0.96	2.56	3.417(4)	149	1/2-x,3/2-y,1-z

Table S5 Equilibrium solubility of pure 2,4-D and its multicomponent crystals in the water at 25°C.

Component	Solubility (g/L)
2,4-D	0.6914 ± 0.0039
(2,4-D) ⁻ (PZ) ⁺	2.7417 ± 0.0118
(2,4-D) ⁻ (BZ) ⁺	2.4590 ± 0.0094
(2,4-D) ⁻ (ABA) ⁺	1.0464 ± 0.0062
(2,4-D) ⁻ (PPD) ⁺	0.6350 ± 0.0031
(2,4-D) ⁻ (OPD) ⁺	1.6883 ± 0.0088
2,4-D-EB	0.3828 ± 0.0008

Table S6 The water solubilities of the coformers of all salts.

Compounds	solubility (g/L)
PZ ⁵	190.7 (25°C)
BZ ⁶	7.6 (25°C)
ABA ⁷	5.9 (25°C)
PPD ⁸	47.2 (25°C)
OPD ⁹	40.4 (35°C)

Table S7 The pH of a saturated solution at 25°C.

Solution	Final pH
pure water	7.18
2,4-D	3.00
(2,4-D) ⁻ (PZ) ⁺	4.86
(2,4-D) ⁻ (BZ) ⁺	4.76
(2,4-D) ⁻ (ABA) ⁺	3.51
(2,4-D) ⁻ (PPD) ⁺	3.53
(2,4-D) ⁻ (OPD) ⁺	4.37
2,4-D-EB	3.20

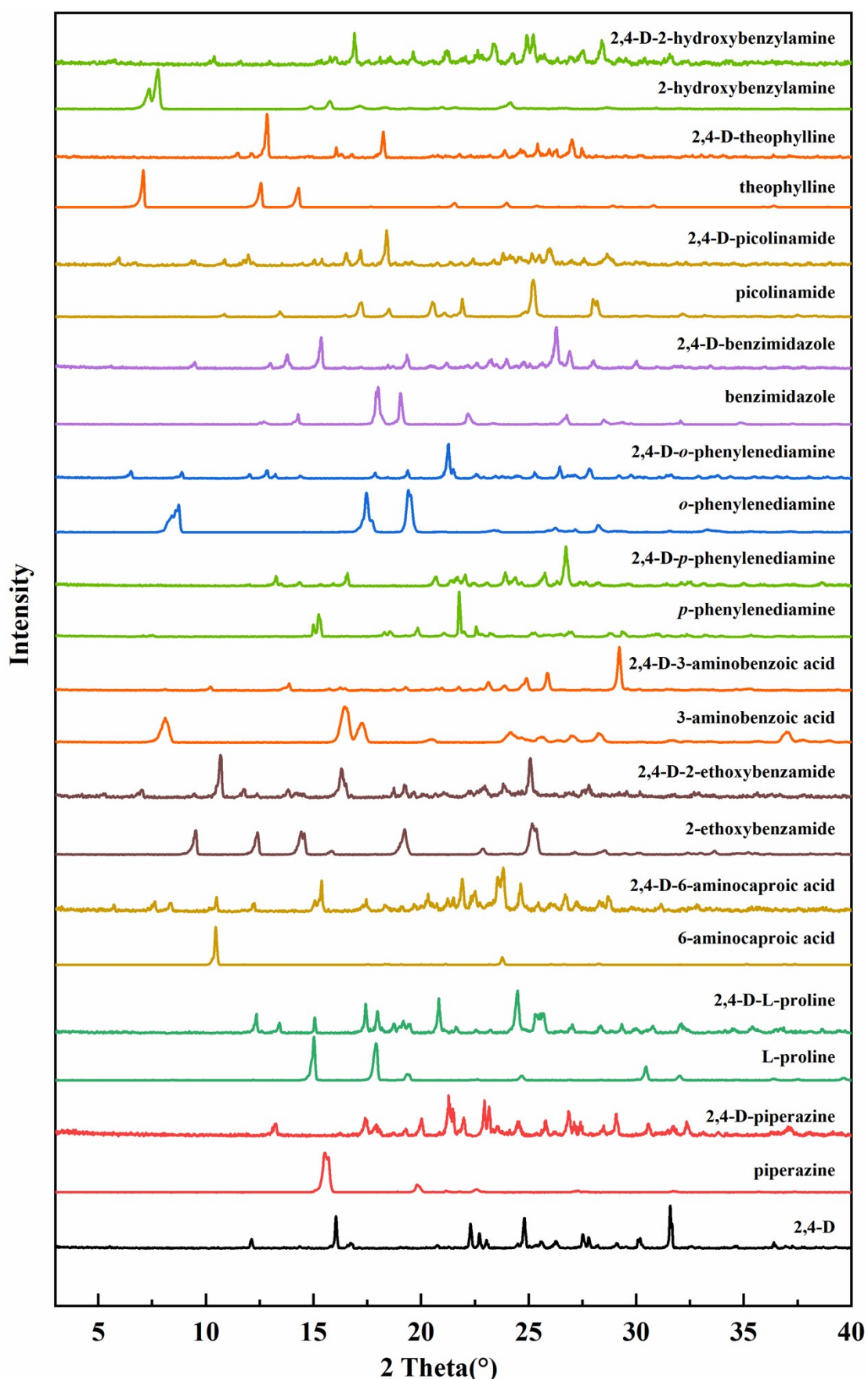


Figure S1 PXRD patterns of LAG experiment product with new phases.

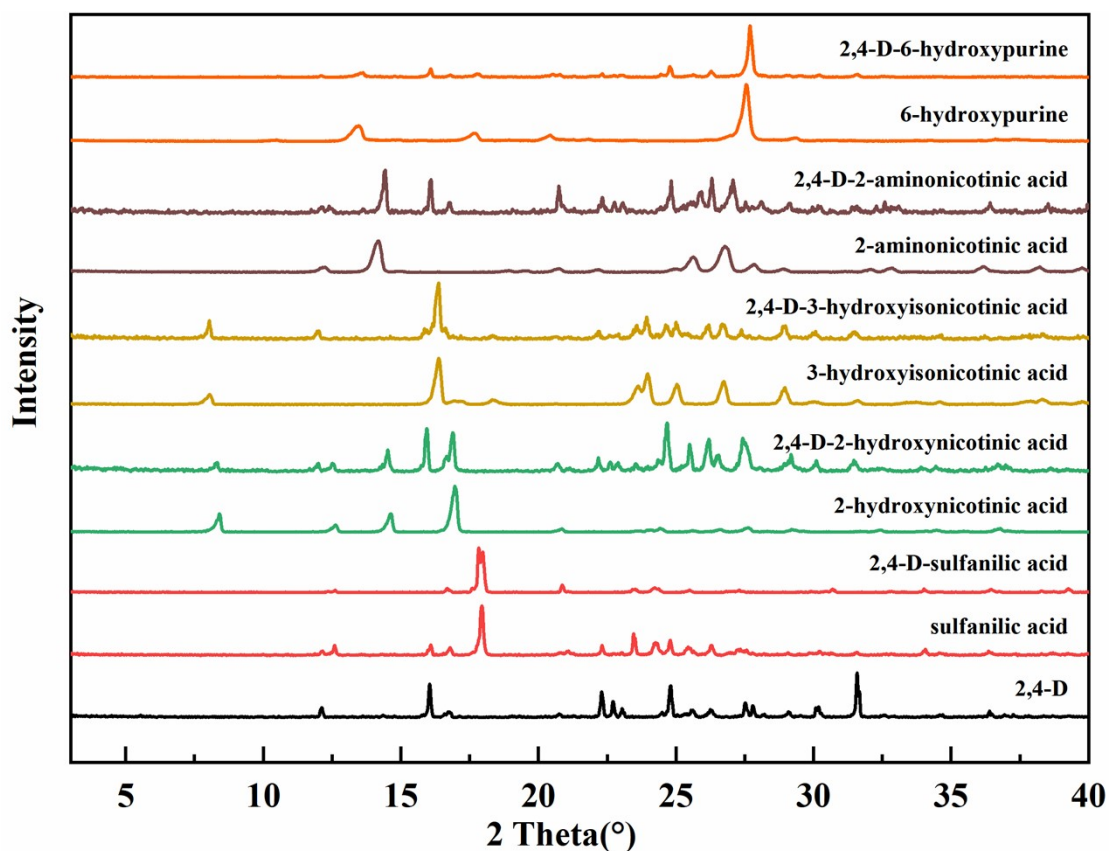


Figure S2 PXRD patterns of LAG experiment product without new phases.

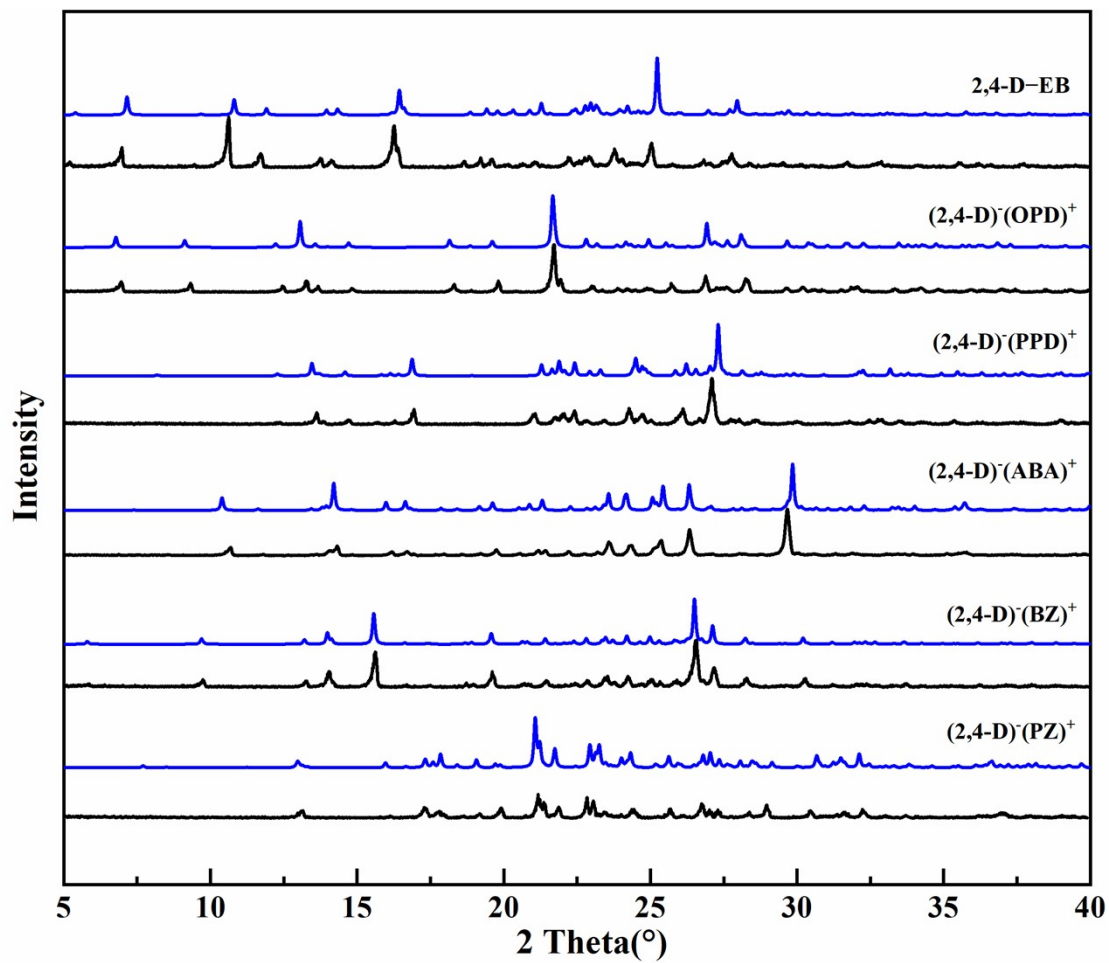


Figure S3 PXRD patterns of multicomponent crystals (black and blue represent the results of slurry suspension experiments and software calculations, respectively).

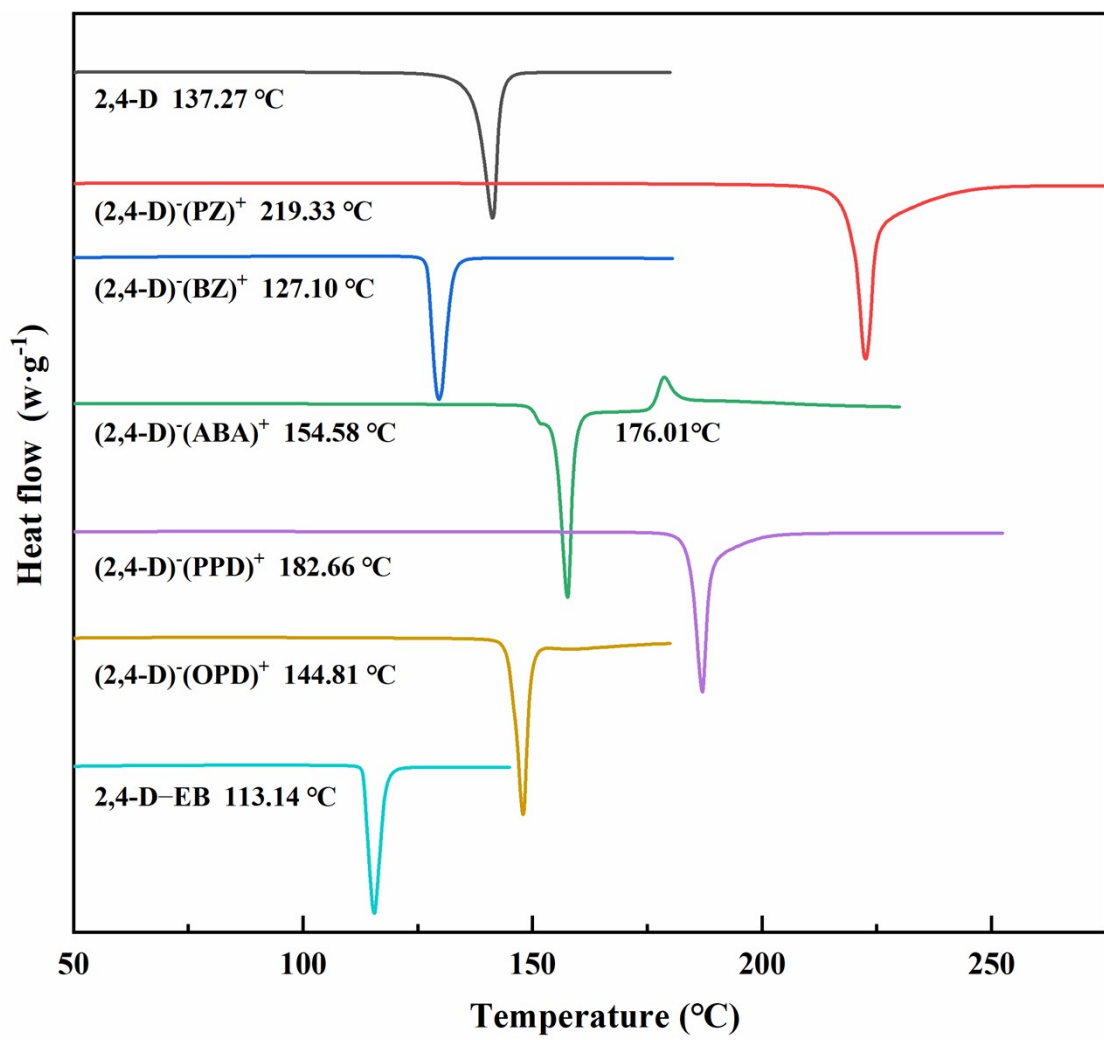


Figure S4 DSC curves of 2,4-D, $(2,4\text{-D})\cdot(\text{PZ})^+$, $(2,4\text{-D})\cdot(\text{BZ})^+$, $(2,4\text{-D})\cdot(\text{ABA})^+$, $(2,4\text{-D})\cdot(\text{PPD})^+$, $(2,4\text{-D})\cdot(\text{OPD})^+$, and 2,4-D-EB.

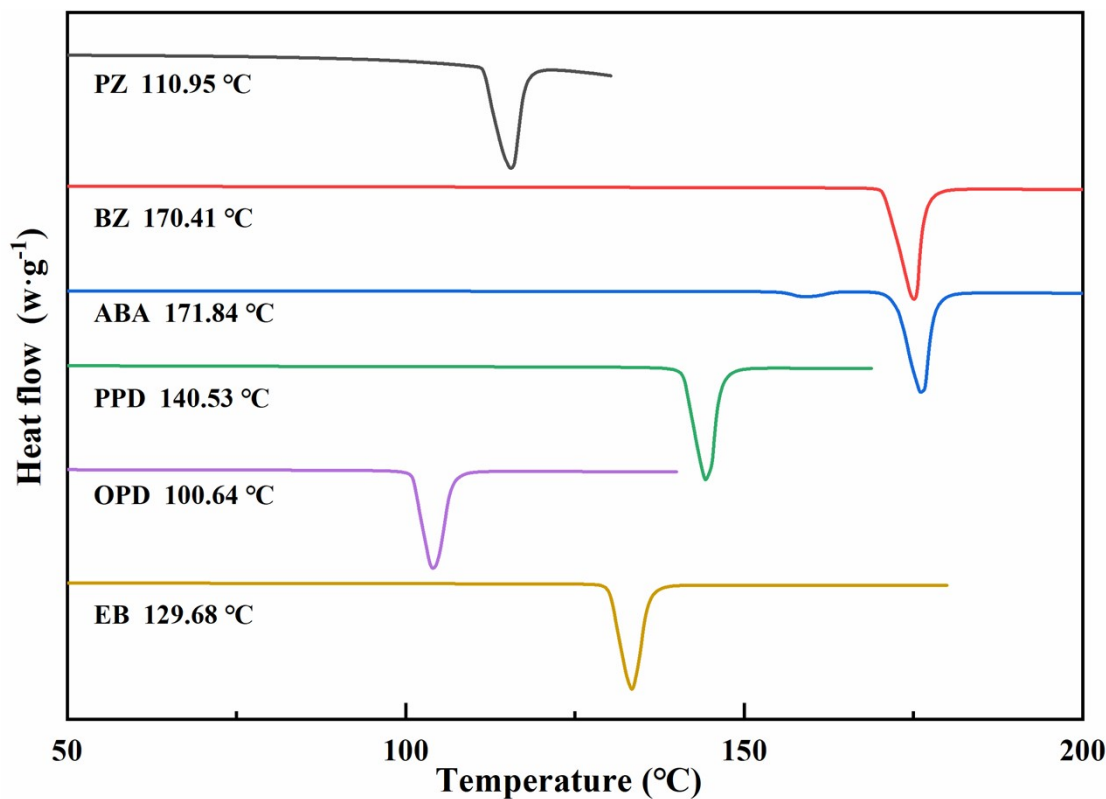


Figure S5 DSC curves of coformers in all multicomponent crystals.

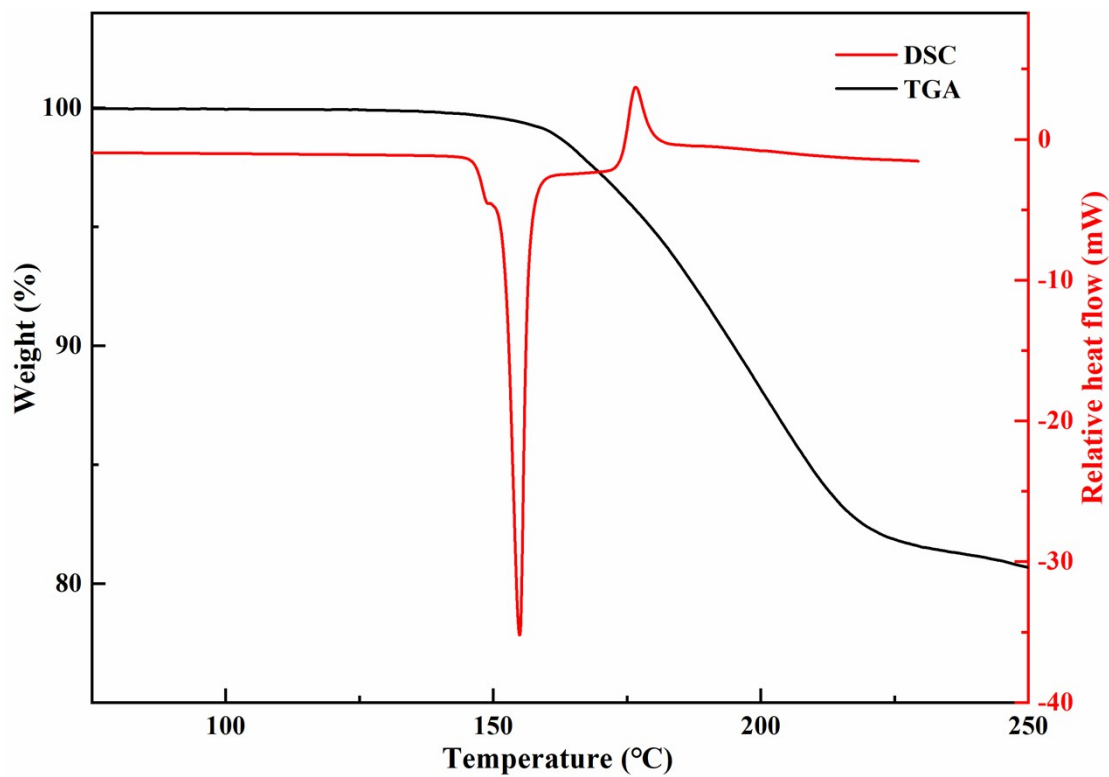


Figure S6 TGA and DSC curves of (2,4-D)-(ABA)⁺.

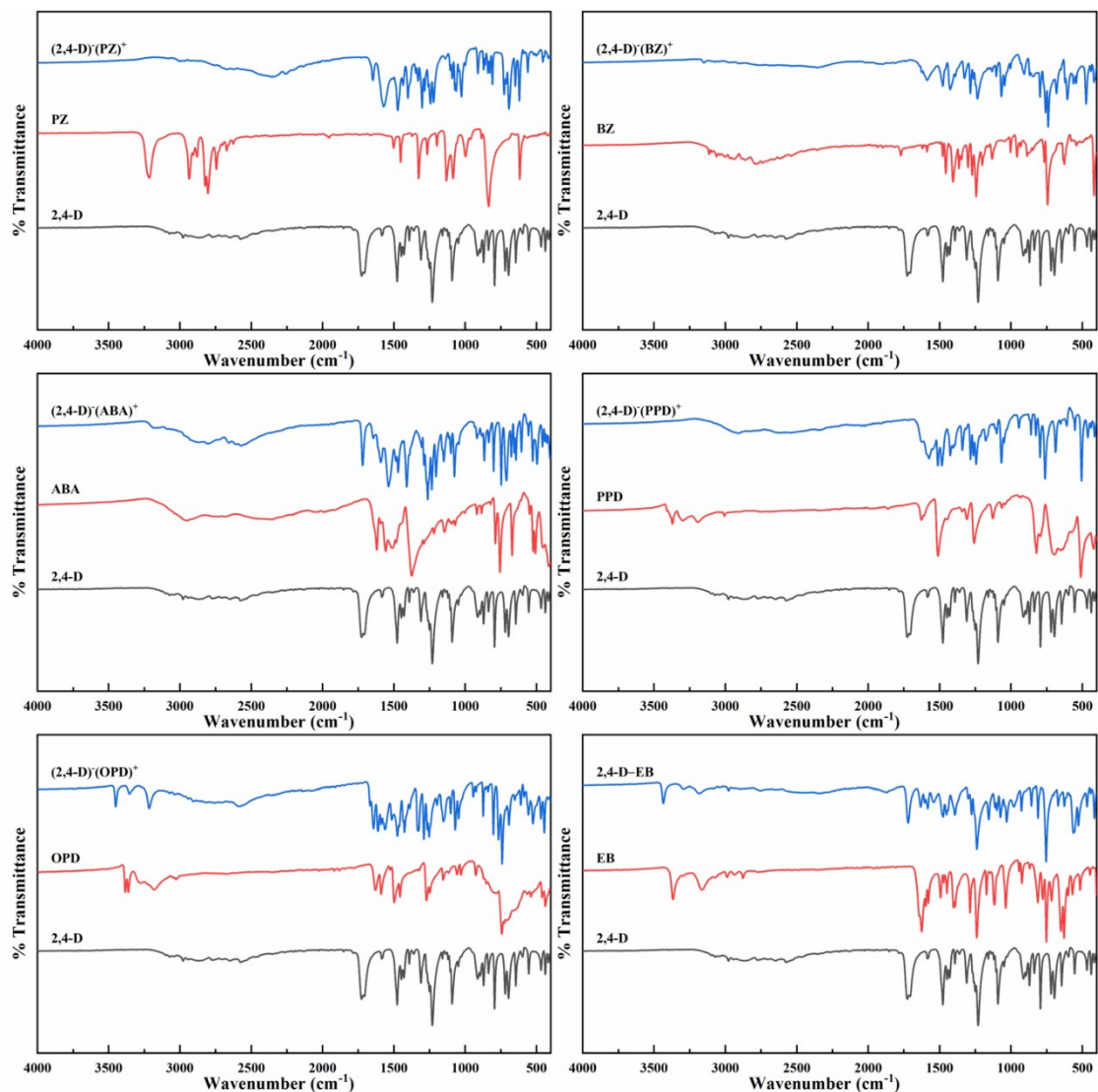


Figure S7 FTIR spectra of the starting materials and multicomponent crystals.

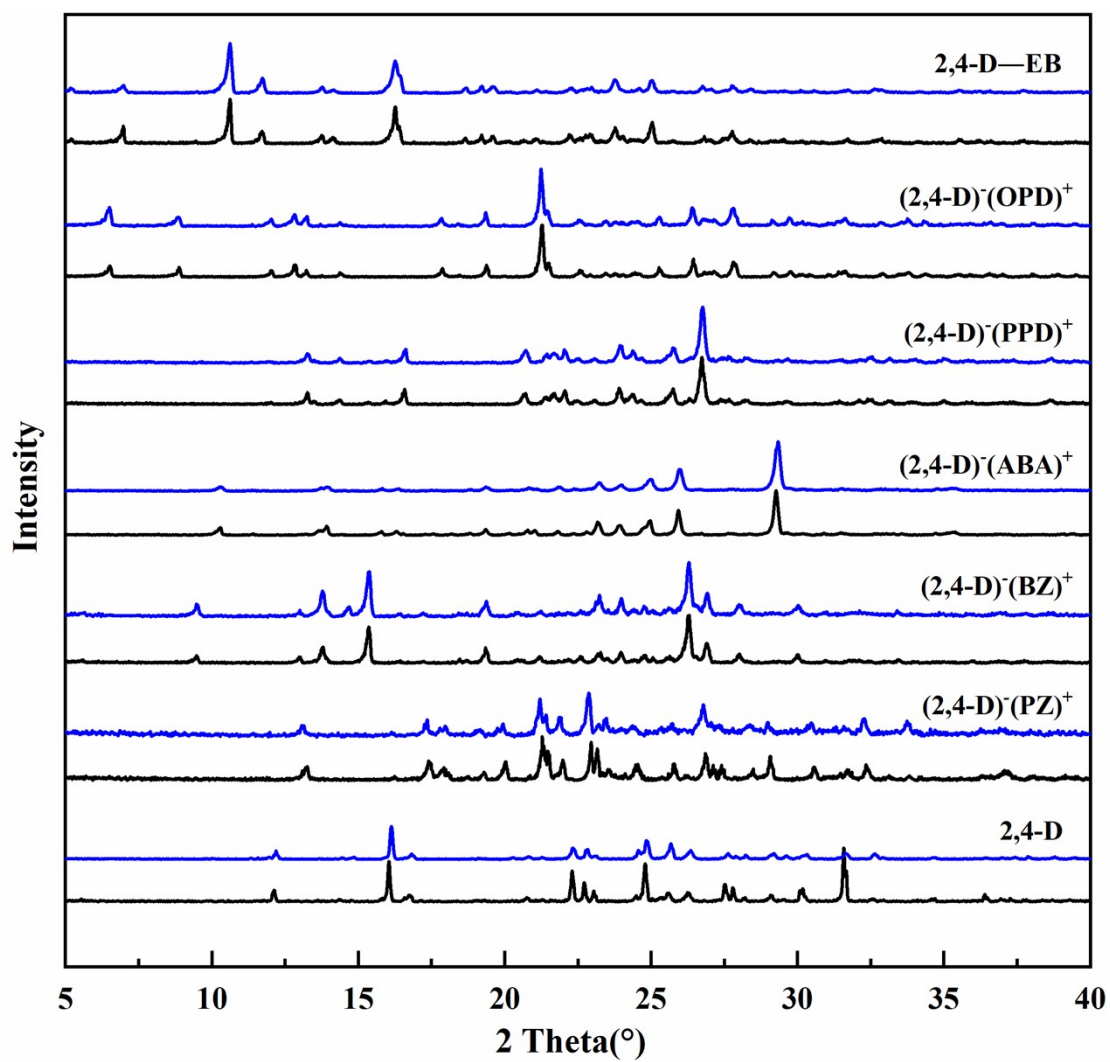


Figure S8 The PXRD patterns of 2,4-D and multicomponent crystals before (black) and after (blue) equilibrium solubility experiment.

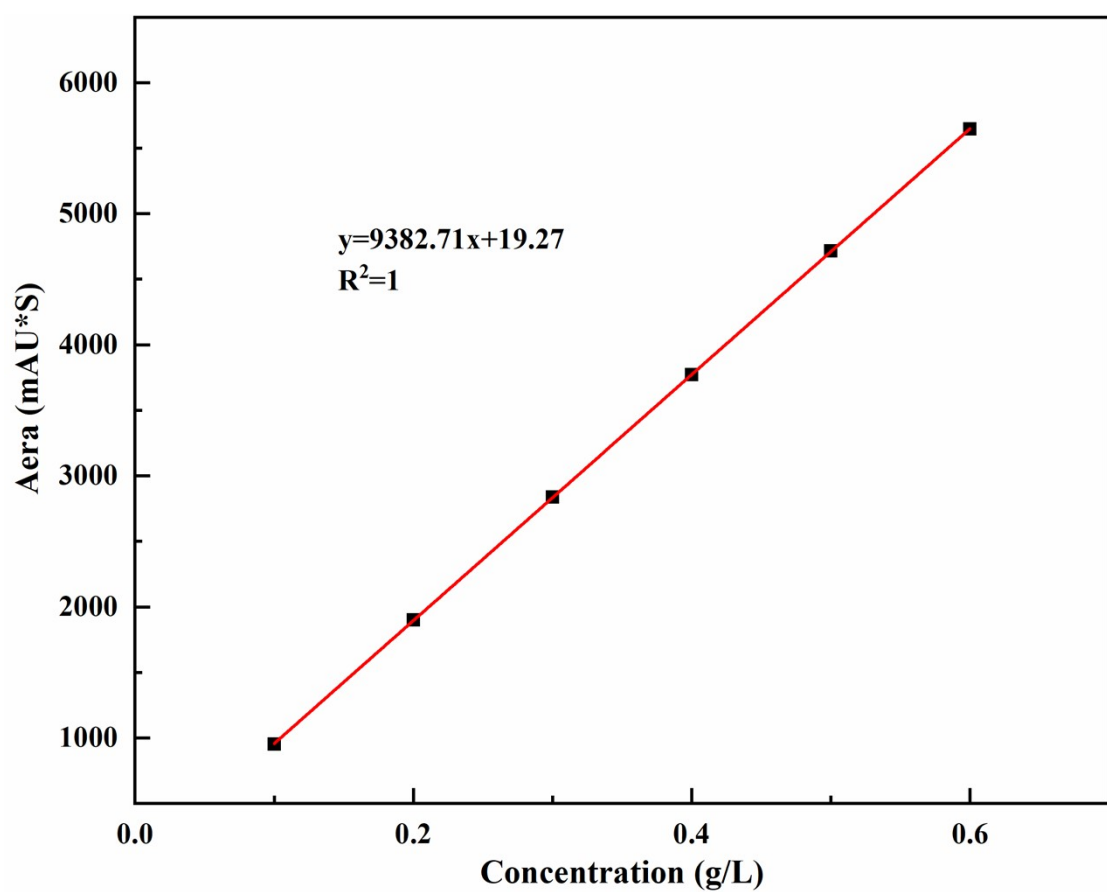


Figure S9 The standard curve of pure 2,4-D solubility.

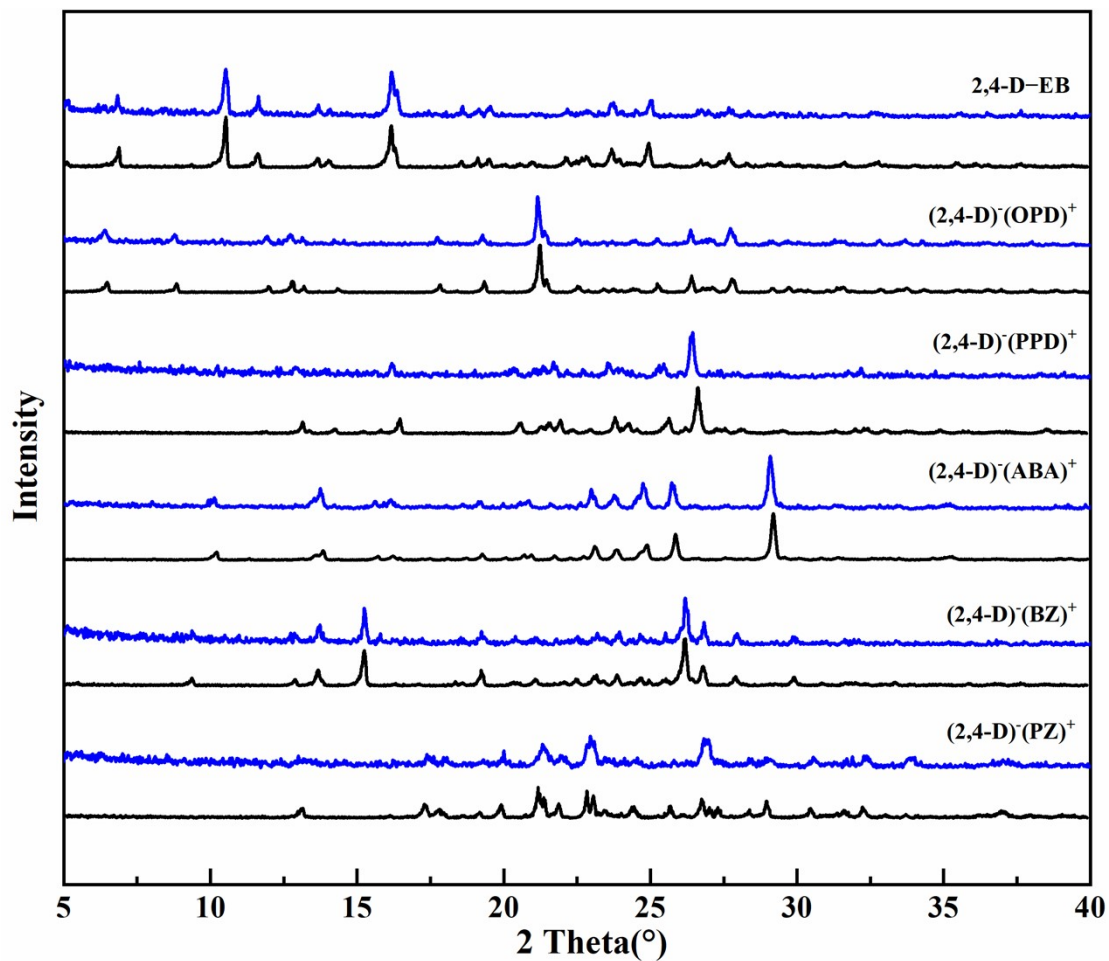


Figure S10 The PXRD patterns of 2,4-D and multicomponent crystals before (black) and after (blue) accelerated stability experiment.

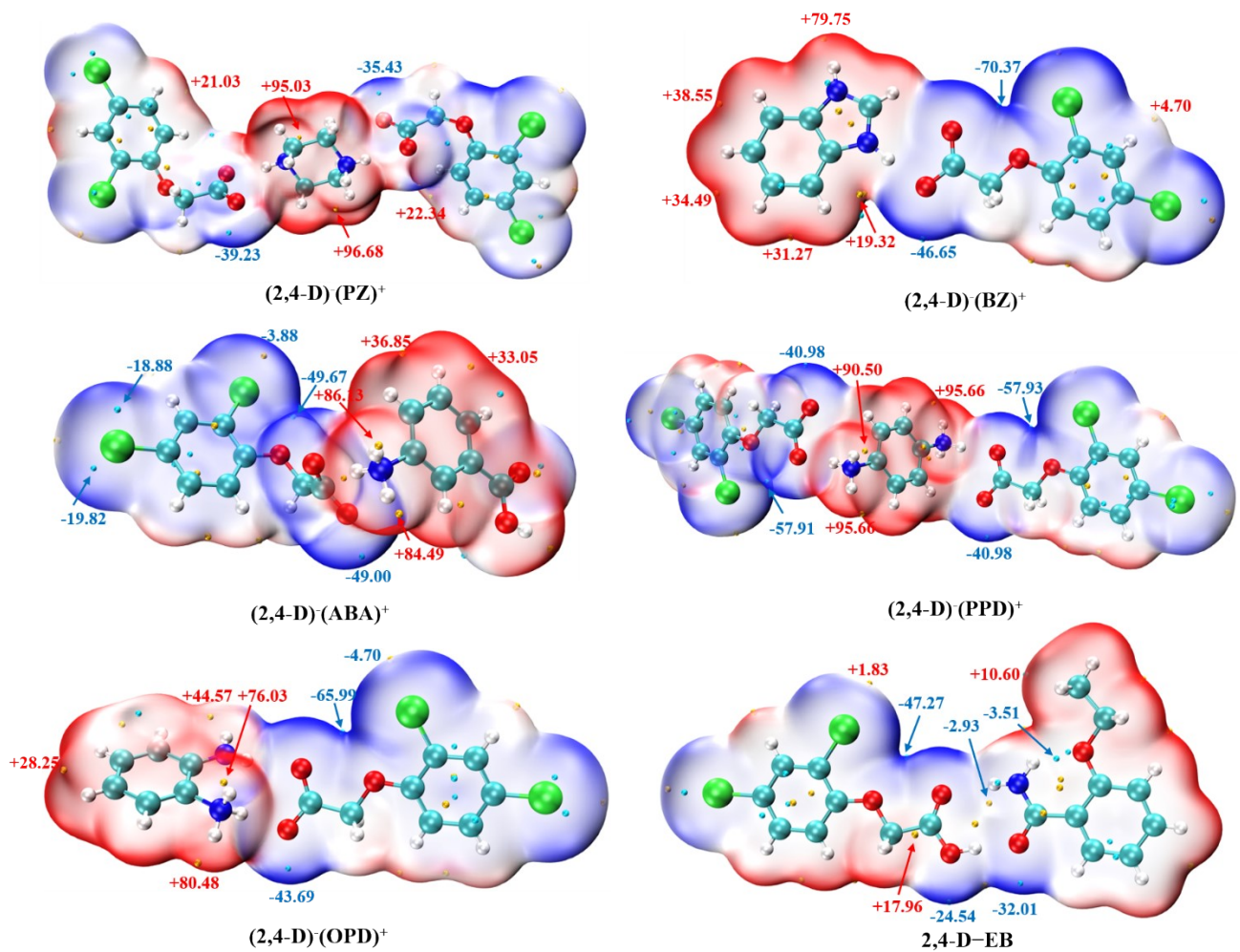


Figure S11 The MEPs of multicomponent crystals.

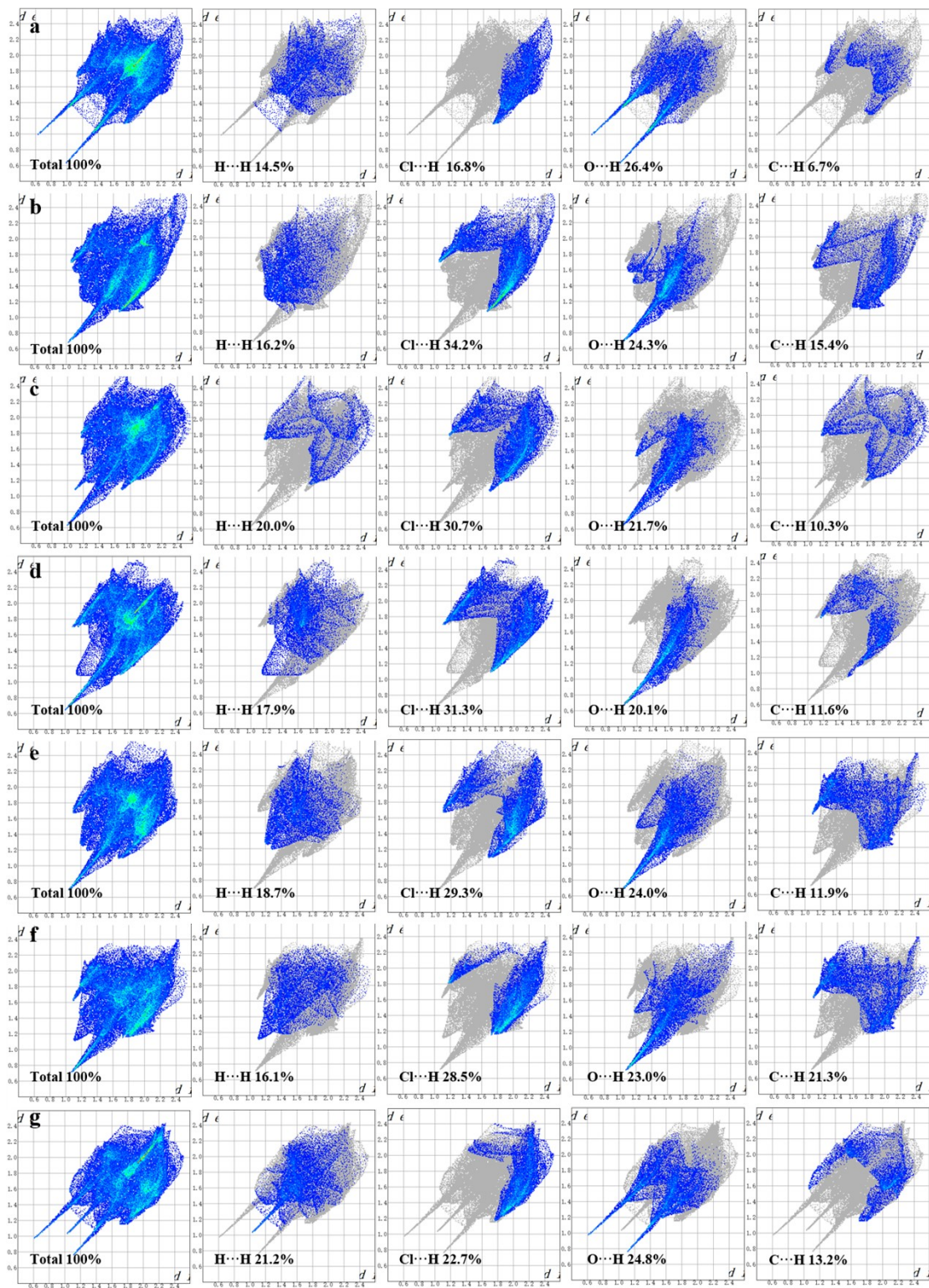


Figure S12 Hirshfeld 2D fingerprint plots of 2,4-D and multicomponent crystals.

1. D. E. Lynch, C. J. Cooper, V. Chauhan, G. Smith, P. Healy and S. Parsons, *Australian Journal of Chemistry*, 1999, **52**, 695-703.

2. L. Fang, Y. Ma, Y. Xiao, Z. Li, Z. Gao, S. Wu, S. Rohani and J. Gong, *Crystal Growth & Design*, 2022, **22**, 1707-1719.
3. L. Fang, Y. Xiao, C. Zhang, Z. Gao, S. Wu, J. Gong and S. Rohani, *Crystengcomm*, 2021, **23**, 7615-7627.
4. D. E. Lynch, T. Latif, G. Smith, K. A. Byriel and C. H. L. Kennard, *Journal of Chemical Crystallography*, 1997, **27**, 567-575.
5. U. Mandal, S. Bhattacharya, K. Das and K. K. Kundu, *Zeitschrift Für Physikalische Chemie*, 1988, **159**, 21-36.
6. <http://www.chemspider.com/Chemical-Structure.5593.html?rid=a535bf87-4740-42b9-8e6c-6c3e75154161>
7. B. Saikia, P. Bora, R. Khatioda and B. Sarma, *Crystal Growth & Design*, 2015, **15**, 5593-5603.
8. Kruyt; Robinson, *Chemisches Zentralblatt*, 1927, **98**, 1117.
9. <http://www.chemspider.com/Chemical-Structure.13837582.html?rid=3a667ebe-d12b-4a90-a648-9a3af38daf47>